Supporting Information

Tuning Conjugated Chain Ends in Small Molecular Acceptors for Enhancing Molecular Packing in Binary Blend acceptors and Inducing High Efficiency in Planar Junction Organic Photovoltaics

Tzu-Ching Lu[a], Bin Chang[a], Chi-Ting Huang[a], Jui-Cheng Kao[a], Bo-Han Chen[b], Ching-En Tsai[a], Chung-Hao Chen[a], Shang-Da Yang[b], Jyh-Pin Chou[c], Yu-Chieh Lo[a] and Kung-Hwa Wei[a]*

a. Department of Materials Science and Engineering, National Yang Ming Chiao Tung University, Hsinchu 30010, Taiwan.

b. Institute of Photonics Technologies, National Tsing Hua University, Hsinchu 300044, Taiwan

c. Graduate School of Advanced Technology, National Taiwan University, Taipei, Taiwan

Characterizations

UV–vis absorption and transmittance spectra were obtained using a Hitachi U-4100 spectrophotometer. The current density–voltage (*J–V*) characteristics were measured with a Keithley 2400 source meter under simulated AM 1.5G illumination (100 mW cm^{-2}), provided by a 150 W xenon lamp-based solar simulator. Light intensity was calibrated using a silicon photodiode equipped with a KG-5 optical filter. EQE spectra were recorded using a commercial system from Enlitech (Taiwan), employing a calibrated mono-silicon photodiode with a spectral response range of 300-1000 nm as the reference detector. Photocurrent density (J_{ph}) was analyzed as a function of effective voltage ($V_{eff} = V_0 - V$), where V_o is defined as the voltage at which J_{ph} equals zero, and J_{sat} corresponds to the saturation photocurrent density. Surface morphology of the films was characterized in tapping mode using atomic force microscopy (AFM; Veeco Innova) under ambient conditions. Transient absorption (TA) measurements were carried out using a custom-built pump–probe setup with 850 nm excitation and a probe range spanning 550–1000 nm. GIWAXS experiments were performed at the 25A beamline (20 keV) at the National Synchrotron Radiation Research Center (NSRRC) in Hsinchu, Taiwan, with an incident angle of 0.02°. For GIWAXS characterization, active layers were spin-coated onto silicon substrates to ensure film uniformity and reliable structural analysis.

Synthetics and materials

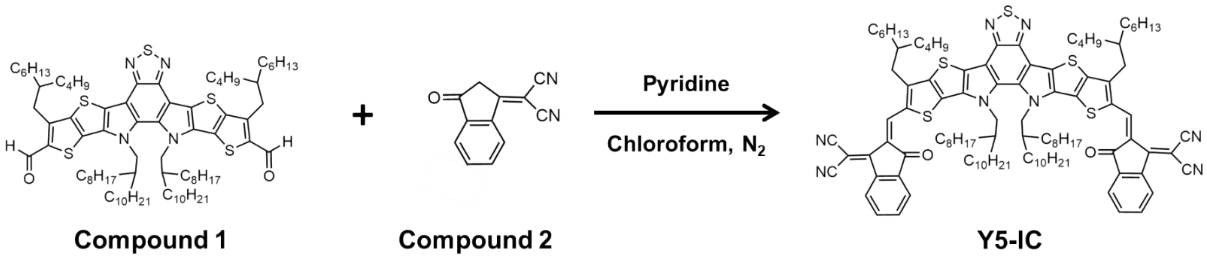

Figure S1. The synthesis process of the Y5-IC.

The reaction was initiated by combining the starting material with 50 mL of dry chloroform ($CHCl_3$) containing 5 mL of pyridine. Subsequently, Compound 1 (BTP-CHO, 200 mg, 0.144 mmol) and Compound 2 (IC-2H, 279.4 mg, 1.44 mmol) were added to the solution. The mixture was refluxed for 4 hours at 100 °C. Upon completion, the reaction mixture was concentrated using a rotary evaporator, and the crude product was purified by silica gel column chromatography using a gradient eluent of hexanes to $CHCl_3$/hexanes (1:2, v/v), affording the target compound Y5-IC. ^{1}H NMR (500 MHz, CDCl3) δ (ppm): 9.18 (s, 2H), 8.73-8.72 (d, 2H), 7.96-7.94 (d, 2H), 7.79-7.74 (m, 4H), 4.77-4.76 (d, 4H), 3.20-3.19 (d, 4H), 2.14-2.09 (m, 4H), 1.51-1.37 (m, 16H), 1.32-1.24 (m, 20H), 1.21-1.18 (m, 4H), 1.16-1.12 (m, 18H), 1.04-0.97 (m,34H), 0.89-0.77 (m, 28H)

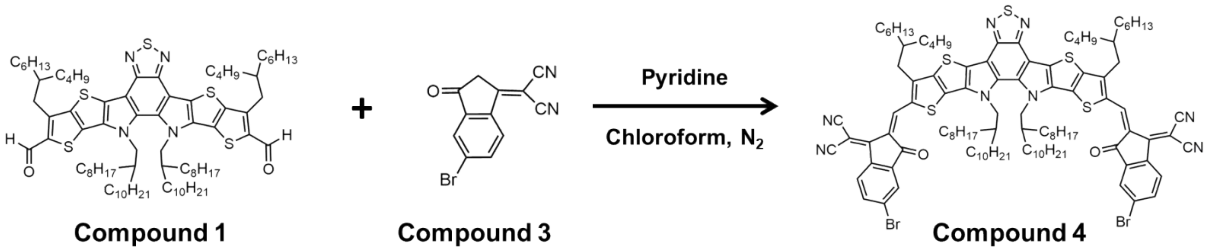

Figure S2. The synthesis process of the Y5-IC-Br (Compound 4).

The reaction was initiated by combining the starting material with 50 mL of dry chloroform ($CHCl_3$) containing 5 mL of pyridine. Subsequently, Compound 1 (BTP-CHO, 200 mg, 0.144 mmol) and Compound 3 (IC-Br, 117.7 mg, 0.432 mmol) were added to the solution. The mixture was then refluxed at 100 °C for 7 hours. Upon completion, the reaction mixture was concentrated using a rotary evaporator, and the crude product was purified by silica gel column chromatography using a gradient eluent of hexanes to $CHCl_3$/hexanes (1:2, v/v), affording the target compound Y5-IC-Br (Compound 4). ^{1}H NMR (500 MHz, CDCl3) δ (ppm): 9.18 (s, 2H), 8.58-8.56 (d, 2H),8.04-8.03 (d, 2H), 7.87 7.86 (m, 2H), 4.78-4.76 (d, 4H), 3.19-3.18 (d, 4H), 2.12-2.09 (m, 4H), 1.49-1.46 (m, 4H), 1.43 1.35 (m, 10H), 1.29-1.20 (m, 30H), 1.17-1.10 (m, 20H), 1.02-0.99 (m, 26H), 0.88-0.78 (m, 30H)

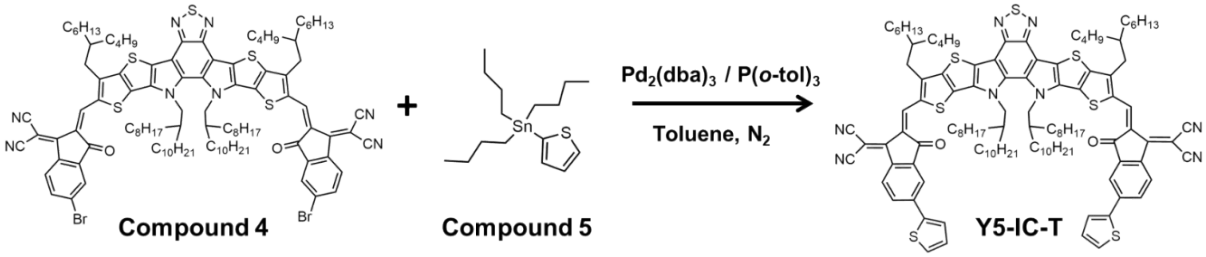

Figure S3. The synthesis process of the Y5-IC-T.

The reaction was initiated by combining the starting material with 15 mL of anhydrous toluene (C_7H_8) containing $Pd_2(dba)_3$ (0.48 mg) and P(*o*-tol)$_3$ (0.64 mg). Subsequently, Compound 4 (Y5-IC-Br, 50mg, 0.026 mmol) and Compound 5 (2-(Tributylstannyl) thiophene, 29.4 mg, 0.078 mmol) were added to the solution. The mixture was then refluxed at 100 °C for 24 hours. Upon completion, the reaction mixture was concentrated using a rotary evaporator, and the crude product was purified by silica gel column chromatography using a gradient eluent of hexanes to $CHCl_3$/hexanes (1:2, v/v), affording the target compound Y5-IC-T. ^{1}H NMR (500 MHz, CDCl3) δ (ppm): 9.16 (s, 2H), 8.71-8.70 (d, 2H),8.14 (d, 2H), 7.98-7.97 (m, 2H), 7.59-7.58 (d, 2H), 7.26-7.19 (m, 2H), 4.78-4.77 (d, 4H), 3.19-3.18 (d, 4H), 2.15-2.098 (m, 4H), 1.52-1.46 (m, 4H), 1.43-1.36 (m, 8H), 1.33-1.24 (m, 24H), 1.19-1.10 (m, 24H),1.02 0.98 (m, 30H) 0.89-0.75 (m, 30H)

Figure S4. The synthesis process of the Y5-IC-TT.

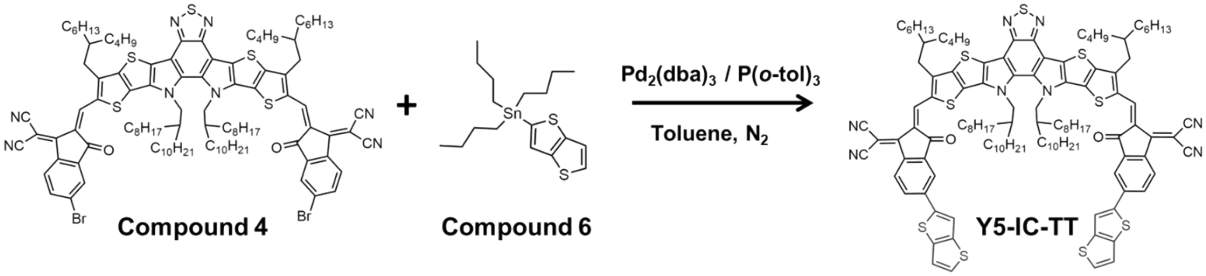

The reaction was initiated by combining the starting material with 15 mL of anhydrous toluene (C_7H_8) containing $Pd_2(dba)_3$ (0.48 mg) and P(*o*-tol)$_3$ (0.64 mg). Subsequently, Compound 4 (Y5-IC-Br, 50mg, 0.026 mmol) and Compound 6 (5-(tributylstannyl)-2,2'-bithiophene, 33.8 mg, 0.078 mmol) were added to the solution. The mixture was then refluxed at 100 °C for 24 hours. Upon completion, the reaction mixture was concentrated using a rotary evaporator, and the crude product was purified by silica gel column chromatography using a gradient eluent of hexanes to $CHCl_3$/hexanes (1:2, v/v), affording the target compound Y5-IC-TT. ^{1}H NMR (500 MHz, CDCl3) δ (ppm): 9.12 (s, 2H), 8.72-8.70 (d, 2H), 8.11-8.10 (d, 2H), 7.98 7.96 (m, 2H), 7.74 (s, 2H), 7.50-7.49 (d, 2H), 7.30-7.26 (d, 2H) 4.81-4.80 (d, 4H), 3.18-3.16 (d, 4H), 2.18-2.09 (m, 4H), 1.51-1.47 (m, 4H), 1.43-1.37 (m, 10H), 1.33-1.24 (m, 24H), 1.18-1.09 (m, 24H), 1.04-1.00 (m, 30H), 0.89-0.83 (m, 16H), 0.80-0.75 (m, 12H)

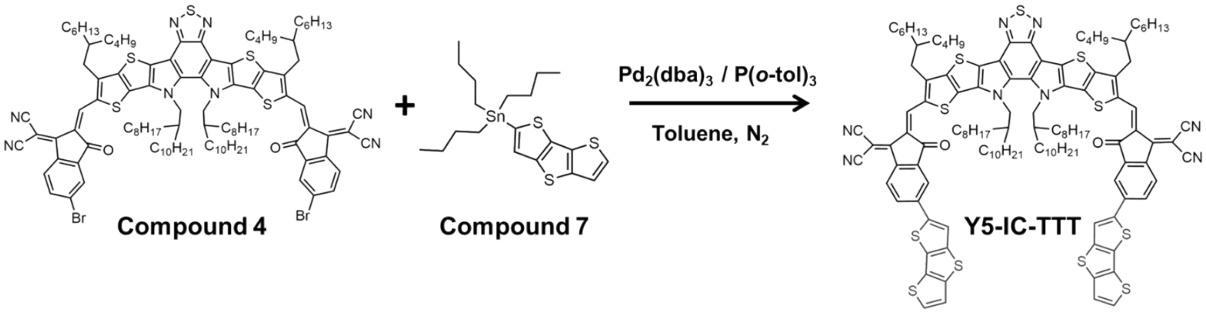

Figure S5. The synthesis process of the Y5-IC-TTT.

The reaction was initiated by combining the starting material with 15 mL of anhydrous toluene (C_7H_8) containing $Pd_2(dba)_3$ (0.48 mg) and P(*o*-tol)$_3$ (0.64 mg). Subsequently, Compound 4 (Y5-IC-Br, 50mg, 0.026 mmol) and Compound 7 (5-(tributylstannyl)thieno[3,2-b]thiophene, 37.8 mg, 0.078 mmol) were added to the solution. The mixture was then refluxed at 100 °C for 24 hours. Upon completion, the reaction mixture was concentrated using a rotary evaporator, and the crude product was purified by silica gel column chromatography using a gradient eluent of hexanes to $CHCl_3$/hexanes (1:2, v/v), affording the target compound Y5-IC-TTT. ^{1}H NMR (500 MHz, CDCl3) δ (ppm): 8.82 (d, 2H), 8.59-8.57 (d, 2H), 7.90 (d, 2H), 7.85 (d, 2H), 7.66 (s, 2H), 7.31-7.30 (d, 2H), 7.26-7.24 (t, 2H), 4.94-4.93 (d, 4H) 2.94-2.93 (m, 4H), 2.29-2.28 (m, 2H), 2.01-1.99 (m, 2H), 1.44-1.32 (m, 16H), 1.28-1.24 (m, 32H), 1.13-1.10 (m, 12H), 1.06-1.02 (m, 30H), 0.93-0.84 (m, 18H), 0.75-0.71 (m, 12H)

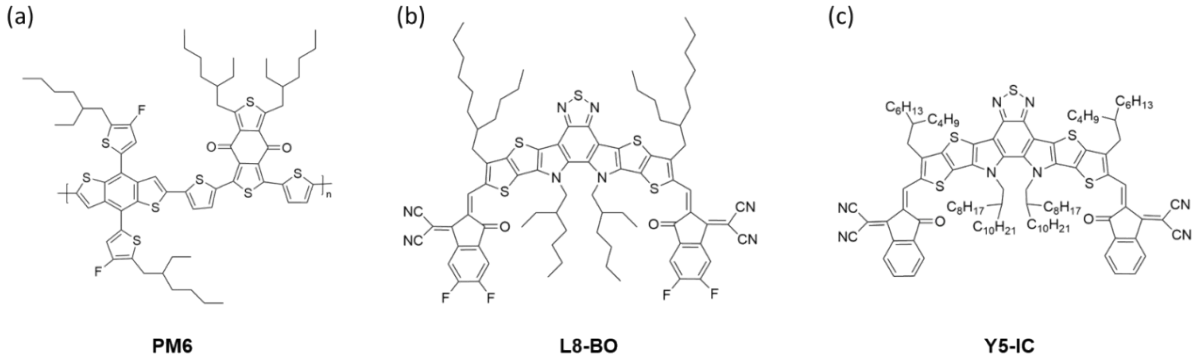

Figure S6. Chemical structures of the (a) polymer donor PM6, (b) small molecule acceptor L8-BO and (c) Y5-IC.

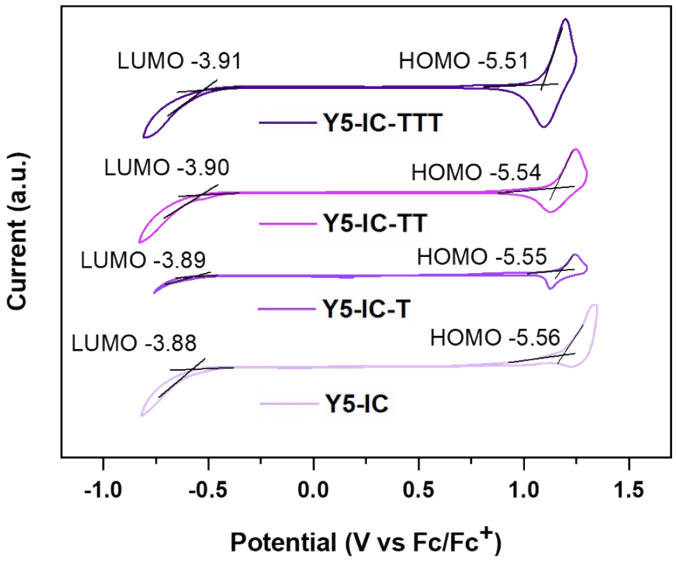

Figure S7. Cyclic voltammetry (CV) of the Y5-IC, Y5-IC-T, Y5-IC-TT and Y5-IC-TTT.

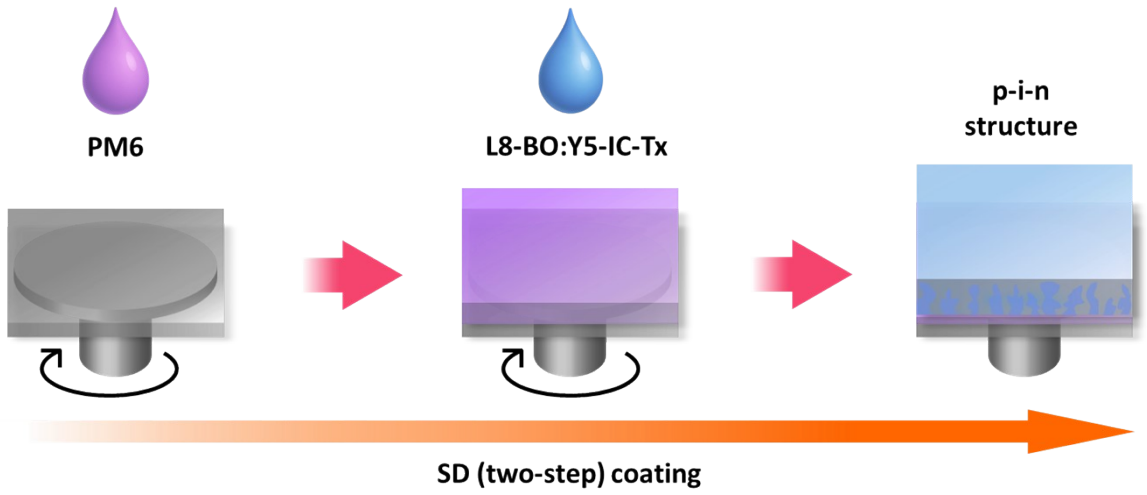

Figure S8. Schematic representation of the sequential deposition process with a spin-coating method and the formation of planar junction.

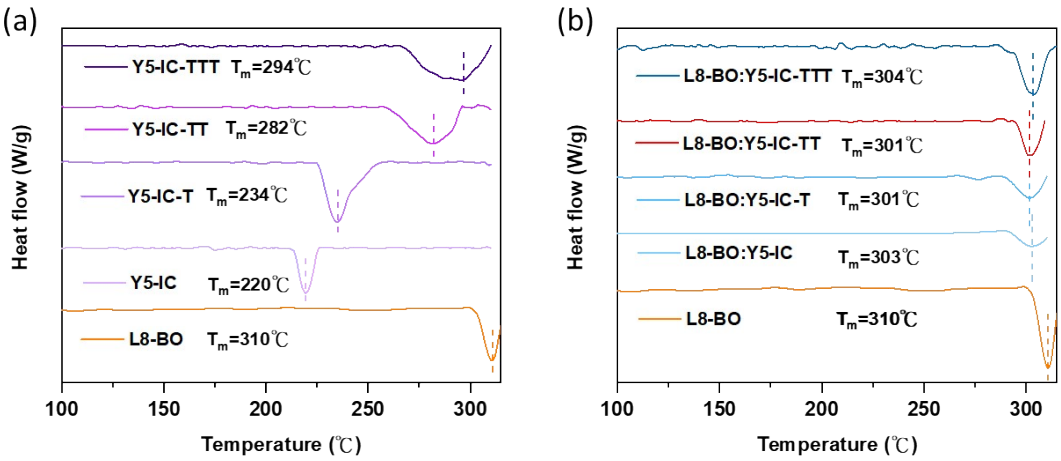

Figure S9. DSC curves of (a) L8-BO, Y5-IC, Y5-IC-T, Y5-IC-TT and Y5-IC-TTT. (b) L8-BO, L8-BO:Y5-IC, L8-BO:Y5-IC-T, L8-BO:Y5-IC-TT, L8-BO:Y5-IC-TTT blend (8:2 by weight) in the heating process.

Figure S10. Contact angle images of PM6, L8-BO, Y5-IC, Y5-IC-T, Y5-IC-TT and Y5-IC-TTT films with water and ethylene glycol droplet on top.

Table S1. Surface energies of the various materials (neat films) and the Flory–Huggins parameters (χ) between them.

Materials (Y)	θ_W [°]	θ_{EG} [°]	Surface energy (mN/m)	$\chi_{L8\text{-}BO/Y}$
PM6	102.8	68.5	33.56	0.034
L8-BO	87.9	64.9	26.87	-
Y5-IC	97.1	70.9	24.09	0.010
Y5-IC-T	98.3	71.4	24.13	0.009
Y5-IC-TT	99.2	71.7	24.30	0.007
Y5-IC-TTT	99.1	72.5	23.66	0.012

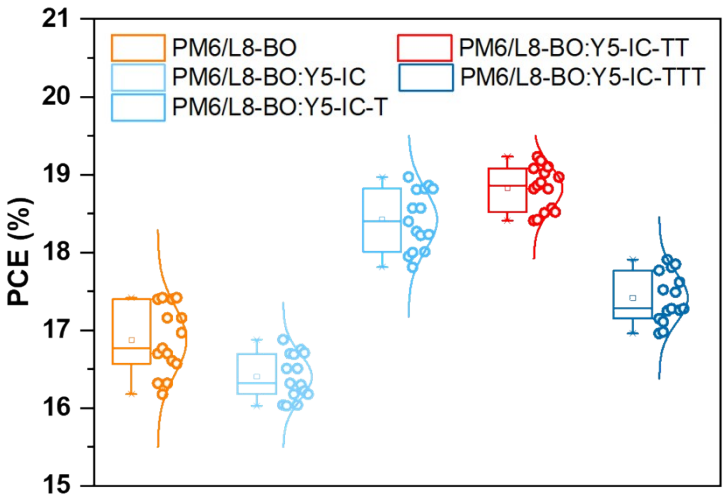

Figure S11. Box plots showing the distributions of the PCE values of PM6 L8-BO SD structure.

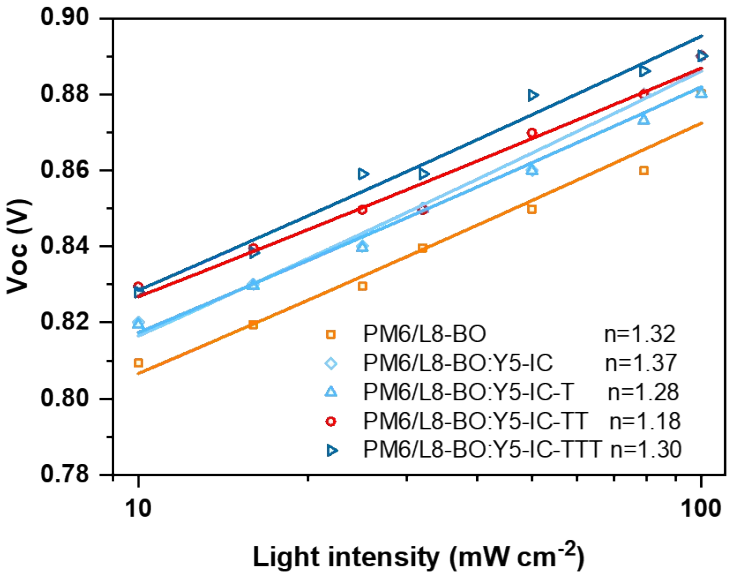

Figure S12. Dependence of *V*oc on light intensity.

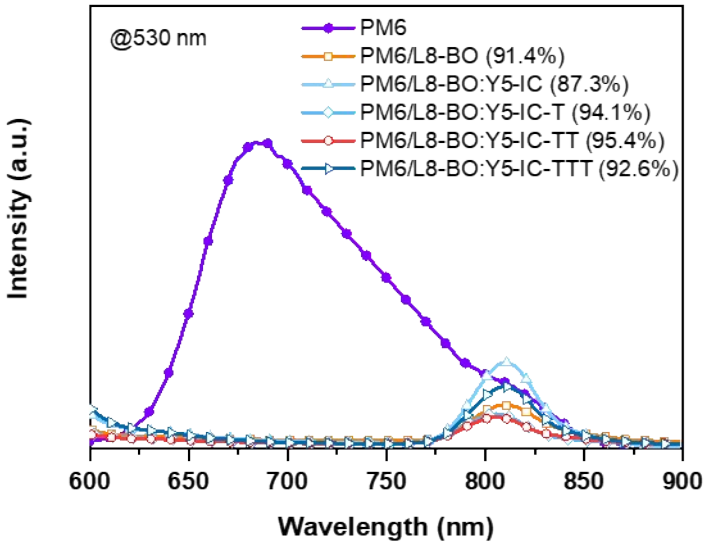

Figure S13. Photoluminescence spectrum of PM6 film; PM6/L8-BO, PM6/L8-BO:Y5-IC, PM6/L8-BO:Y5-IC-T, PM6/L8-BO:Y5-IC-TT, PM6/L8-BO:Y5-IC-TTT blend films.

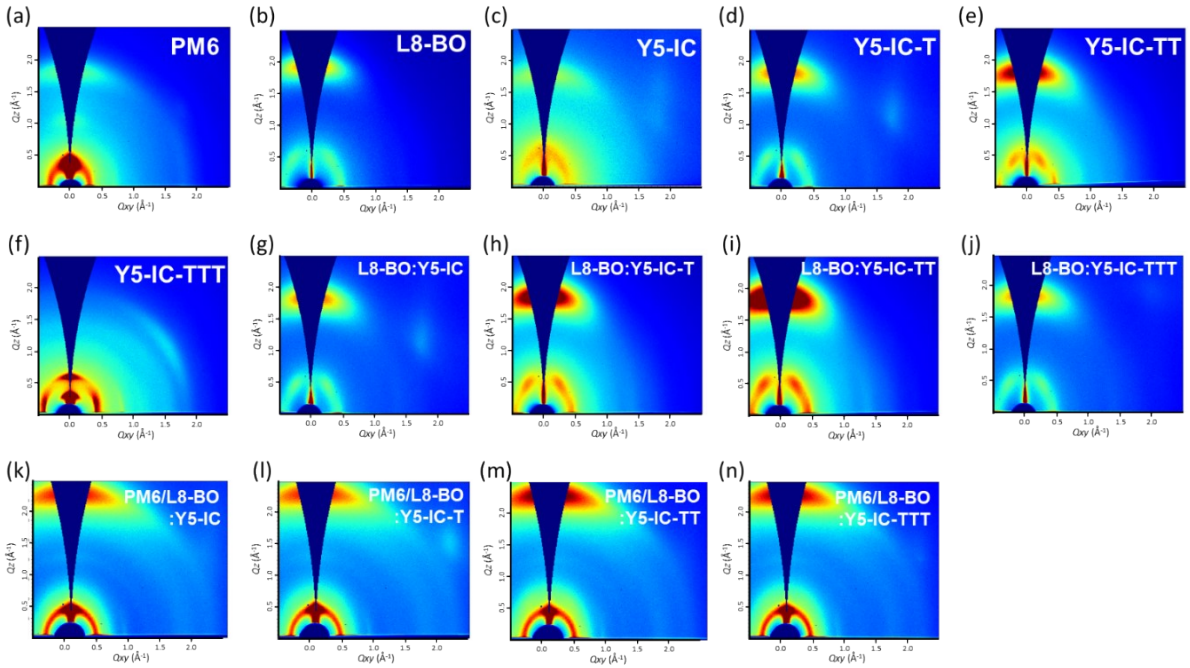

Figure S14. 2D GIWAXS of the pristine films of (a) PM6, (b) L8-BO, (c) Y5-IC, (d) Y5-IC-T, (e) Y5-IC-TT and (f) Y5-IC-TTT. 2D GIWAXS of the binary-acceptor-blend films of (g) L8-BO:Y5-IC, (h) L8-BO:Y5-IC-T, (i) L8-BO:Y5-IC-TT and (j) L8-BO:Y5-IC-TTT. 2D GIWAXS of the planar junction films of (k) PM6/L8-BO:Y5-IC, (l) PM6/L8-BO:Y5-IC-T, (m) PM6/L8-BO:Y5-IC-TT and (n) PM6/L8-BO:Y5-IC-TTT.

Figure S15. Thermal stability of the devices with PM6/L8-BO, PM6/L8-BO:Y5-IC-T, and PM6/L8-BO:Y5-IC-TT active layers under 85 °C.

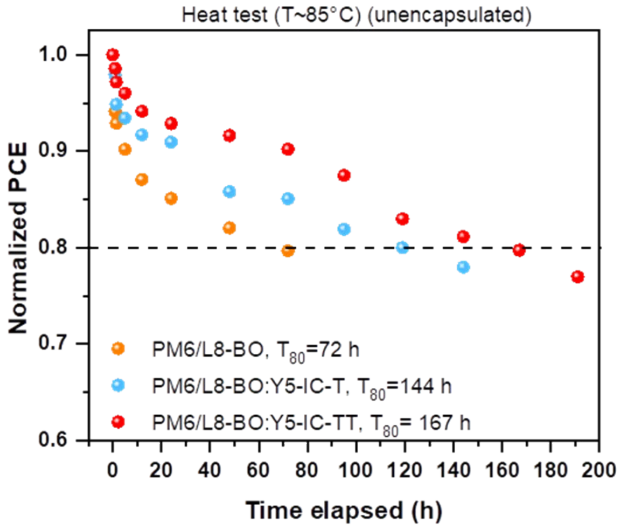

Table S2. The GIWAXS measurements data of the scattering vector q, d-spacing, FWHM, and coherence length (CCL) of films.

Out of plane	q (010) [Å^{-1}]	d (010) [Å]	FWHM (010)[Å^{-1}]	CCL (010) [Å]

PM6	1.78	3.5	0.22	25.7
L8-BO	1.88	3.3	0.33	17.1
Y5-IC	1.74	3.6	0.28	20.2
Y5-IC-T	1.76	3.6	0.27	20.9
Y5-IC-TT	1.79	3.5	0.26	21.7
Y5-IC-TTT	-	-	-	-
L8-BO:Y5-IC	1.80	3.5	0.36	15.7
L8-BO:Y5-IC-T	1.84	3.4	0.33	17.1
L8-BO:Y5-IC-TT	1.84	3.4	0.30	18.8
L8-BO:Y5-IC-TTT	1.82	3.5	0.53	10.7
PM6/L8-BO	1.80	3.5	0.33	17.1
PM6/L8-BO:Y5-IC	1.81	3.5	0.35	16.1
PM6/L8-BO:Y5-IC-T	1.82	3.4	0.33	17.1
PM6/L8-BO:Y5-IC-TT	1.82	3.4	0.33	17.1
PM6/L8-BO:Y5-IC-TTT	1.82	3.4	0.33	17.1

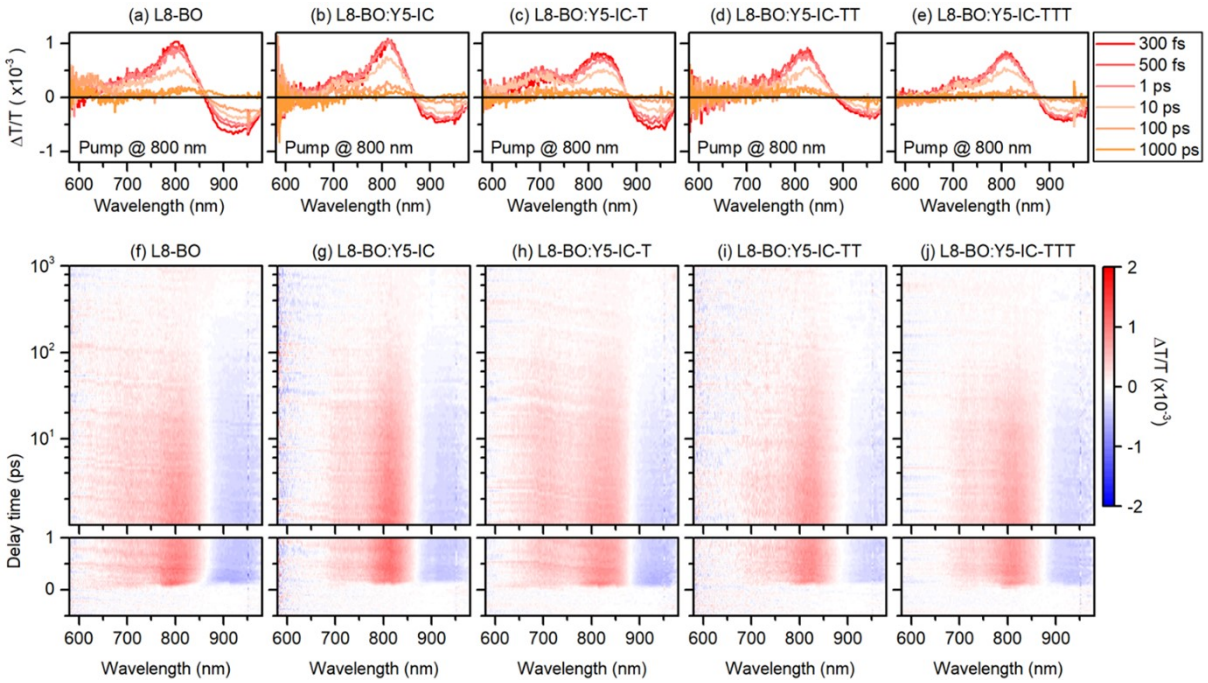

Figure S16. TA spectra at indicated delay time of (a) L8-BO, (b) L8-BO:Y5-IC, (c) L8-BO:Y5-IC-T, (d) L8-BO:Y5-IC-TT, (e) L8-BO:Y5-IC-TTT films pump at 800 nm ; 2D contour plots of the time-resolved TA spectra for (f) L8-BO,(g) L8-BO:Y5-IC, (h) L8-BO:Y5-IC-T, (i) L8-BO:Y5-IC-TT and (j) L8-BO:Y5-IC-TTT films pump at 800 nm.